The major α-tubulin K40 acetyltransferase αTAT1 promotes rapid ciliogenesis and efficient mechanosensation

Toshinobu Shida, Juan G. Cueva, Zhenjie Xu, Miriam B. Goodman[1], and Maxence V. Nachury[1]

Department of Molecular and Cellular Physiology, Stanford University School of Medicine, Stanford, CA 94305-5345

Edited* by Kathryn V. Anderson, Sloan-Kettering Institute, New York, NY, and approved October 20, 2010 (received for review September 15, 2010)

Long-lived microtubules found in ciliary axonemes, neuronal processes, and migrating cells are marked by α-tubulin acetylation on lysine 40, a modification that takes place inside the microtubule lumen. The physiological importance of microtubule acetylation remains elusive. Here, we identify a BBSome-associated protein that we name αTAT1, with a highly specific α-tubulin K40 acetyltransferase activity and a catalytic preference for microtubules over free tubulin. In mammalian cells, the catalytic activity of αTAT1 is necessary and sufficient for α-tubulin K40 acetylation. Remarkably, αTAT1 is universally and exclusively conserved in ciliated organisms, and is required for the acetylation of axonemal microtubules and for the normal kinetics of primary cilium assembly. In *Caenorhabditis elegans*, microtubule acetylation is most prominent in touch receptor neurons (TRNs) and MEC-17, a homolog of αTAT1, and its paralog αTAT-2 are required for α-tubulin acetylation and for two distinct types of touch sensation. Furthermore, in animals lacking MEC-17, αTAT-2, and the sole *C. elegans* K40α-tubulin MEC-12, touch sensation can be restored by expression of an acetyl-mimic MEC-12[K40Q]. We conclude that αTAT1 is the major and possibly the sole α-tubulin K40 acetyltransferase in mammals and nematodes, and that tubulin acetylation plays a conserved role in several microtubule-based processes.

cytoskeleton | posttranslational modification | cilia | Bardet-Biedl Syndrome | ciliopathy

Long-lived, stable microtubules are found inside neuronal processes and cilia and provide stable tracks for motors. Stable microtubules also play essential and conserved roles in the sense of touch and harbor a variety of posttranslational modifications such as detyrosination, polyglutamylation, and N-acetylation of ε-lysines (1). Although most known modifications are displayed on the outside of the microtubule lattice, the major acetylation site in ciliary microtubules is located on lysine-40 of α-tubulin, a residue that points into the lumen of microtubules (2). Thus far, the functional consequences of α-tubulin K40 acetylation have remained perplexing, as genetic alteration of α-tubulin K40 has failed to produce detectable phenotypes in either protozoa (3, 4) or nematodes (5). Nonetheless, recent evidence suggest that kinesin-1 preferentially travels on acetylated microtubule tracks (6, 7) and that α-tubulin K40 acetylation is required for radial glial cell migration (8). These various data have made the physiological role of α-tubulin K40 acetylation subject to debates that have not been resolved because of a lack of tools for eliminating α-tubulin K40 acetylation. In particular, although two α-tubulin K40 deacetylases are known, the identity of the α-tubulin K40 acetyltransferase (αK40 TAT or αTAT) remains unknown (1), despite recent suggestions that some histone acetyltransferases (HATs) and N-acetyltransferases influence microtubule acetylation (9, 10).

Results

A BBSome-Associated Protein Specifically Acetylates Lysine 40 of α-Tubulin in Vitro. We previously showed that a subunit of the BBSome, a ciliary trafficking complex, is required for α-tubulin K40 acetylation (11). Recently, we copurified C6orf134, an uncharacterized protein, together with the BBSome (12), and we confirmed that C6orf134 directly binds to the BBSome (Fig. 1*A*). Intriguingly, C6orf134 is predicted to harbor the GNAT fold found in HATs (13). We thus hypothesized that C6orf134 is the long-sought TAT responsible for K40 acetylation of α-tubulin. To test this assumption, we assayed recombinant C6orf134 for enzymatic transfer of acetyl from acetyl-CoA onto tubulin. Consistent with our hypothesis, we found robust incorporation of radiolabeled acetyl into tubulin—as much as 0.51 mol/mol (Fig. 1*C*)—and a concomitant increase in the immunoreactivity for mAb 6-11B-1 (Fig. 1 *B* and *D*), an antibody that specifically recognizes α-tubulin K40Ac (14). The time courses of [^{14}C]acetyl incorporation and K40Ac synthesis were similar (Fig. 1 *C* and *D*). Similar findings were reported independently (15). C6orf134 was thus renamed αTAT1.

The boundaries of the predicted GNAT fold and of the minimal acetyltransferase domain of αTAT1 are nearly identical (Fig. 1 *E*–*G*), suggesting that the mechanism of acetyl group transfer is conserved between αTAT1 and HATs. To test this idea and to generate a catalytically inactive αTAT1, we searched for conserved acidic residues, as most GNAT family members use an acidic residue for catalysis. We identified D157 and found that αTAT1 [D157N] failed to acetylate purified tubulin (Figs. 1 *F* and *H*). Thus, the TAT activity resides within αTAT1 and not a contaminant.

Recent proteome-wide studies have found multiple acetylated lysines on α- and β-tubulin (16). We therefore tested whether lysines other than α-tubulin K40 are acetylated by αTAT1 in vitro. Although αTAT1 acetylates tubulin purified from WT *Tetrahymena*, it is unable to acetylate tubulin purified from an α-tubulin [K40R] knock-in *Tetrahymena* strain (Fig. 2*A*). Thus, αTAT1 specifically acetylates K40 of α-tubulin. In further support of this conclusion, we calculated that the total amount of acetyl deposited onto tubulin is nearly identical to the amount of acetyl specifically incorporated at K40 of α-tubulin (Fig. 1 *C* and *D*).

All protein lysine acetyltransferases (KAT) identified to date have been HATs, and some HATs acetylate nonhistone substrates (17). To determine the substrate specificity of αTAT1, we incubated recombinant αTAT1 with either recombinant histone H3/H4 (Fig. 2*B*) or purified core histones (Fig. S1*A*) and found that αTAT1 is unable to detectably acetylate any of the core histones, whereas HAT1/RbAp46 efficiently acetylates histone H4 under the same conditions. Furthermore, HAT1/RbAp46 was unable to acetylate tubulin (Fig. S1*A*). Thus, αTAT1 is a KAT that is not a HAT.

Author contributions: T.S., J.G.C., Z.X., M.B.G., and M.V.N. designed research; T.S., J.G.C., Z.X., and M.V.N. performed research; T.S., J.G.C., Z.X., M.B.G., and M.V.N. analyzed data; and M.B.G. and M.V.N. wrote the paper.

The authors declare no conflict of interest.

*This Direct Submission article had a prearranged editor.

See Commentary on page 21238.

[1]To whom correspondence may be addressed. E-mail: mbgoodman@stanford.edu or nachury@stanford.edu.

This article contains supporting information online at www.pnas.org/lookup/suppl/doi:10.1073/pnas.1013728107/-/DCSupplemental.

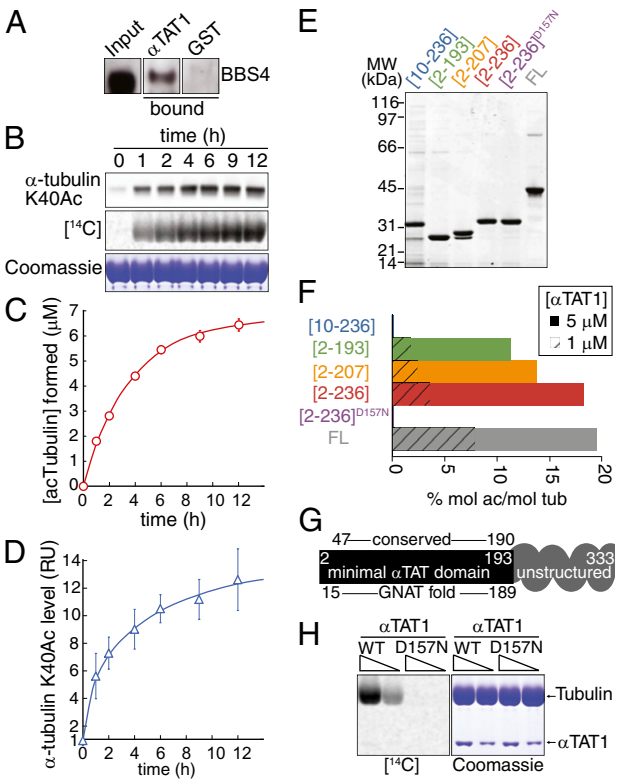

Fig. 1. αTAT1 acetylates tubulin through its GNAT domain in vitro. (*A*) C6orf134/αTAT1 directly binds to the BBSome. GST-αTAT1 and GST were immobilized on beads and mixed with pure BBSome, and bound fractions were immunoblotted for the BBSome subunit BBS4. All panels are from the same film. (*B*) Recombinant αTAT1 efficiently transfers acetyl groups onto K40 of α-tubulin. αTAT1 (1 μM) was mixed with tubulin and [^{14}C]acetylCoA and incubated at 24 °C for the indicated times. Reactions were conducted in triplicate and immunoblotted for α-tubulin K40Ac (*Top*), subjected to phosphorimaging (*Middle*), Coomassie staining (*Bottom*) or filtered to count tubulin-bound radioactivity (plotted in *C*). Coomassie-stained gel shows α/β-tubulin (thick band) and αTAT1 (thin band). (*C* and *D*) Time course of acTubulin and αK40Ac formation. Filter-bound radioactivity representing acetyl groups transferred to tubulin was counted and used to calculate the absolute amount of acetylated tubulin (*C*). At the final time point, the acetylation level reached 0.51 ± 0.02 mol acetyl per mol tubulin. Immunoblot signals were quantified and normalized to the signal intensity at time 0 (*D*). The level of αK40Ac is increased 12.6-fold at end of reaction. Because ~5% of bovine brain α-tubulin is acetylated at K40 (42), we calculate that 0.58 ± 0.13 mol of acetyl are transferred to K40 per mol tubulin after 12 h. Error bars are SD and are smaller than some symbols. (*E*) Purified αTAT1 variants. A 2-μg quantity of each αTAT1 variant was resolved by SDS/PAGE and the gel stained with Coomassie. αTAT1[10-236] is likely to be partially unfolded and contaminated with chaperones. (*F*) Activity of αTAT1 variants. 1 μM (hatched bars) or 5 μM (solid bars) of each αTAT1 variants were incubated with tubulin and [^{3}H] acetylCoA for 1 h at 24 °C and acetyl incorporation into tubulin measured by filter assay. (*G*) Summary diagram of truncation study, structural predictions (13), and sequence conservation. The minimal αTAT domain extends N-terminally from predicted GNAT fold, whereas the unstructured and poorly conserved C terminus of αTAT1 enhances catalytic efficiency. (*H*) Aspartate D157 is crucial for αTAT1 enzymatic activity. Either 5 or 2.5 μM αTAT1[2-236] or αTAT1[2-236]^{D157N} was incubated with tubulin as in *B*. No radiolabel incorporation was detected with αTAT1[2-236]^{D157N}.

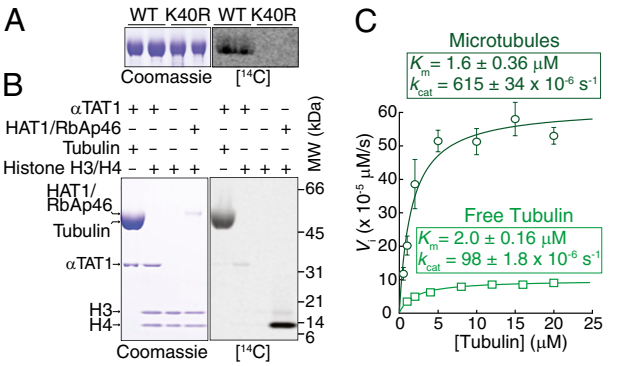

Fig. 2. αTAT1 specifically acetylates K40 of α-tubulin and prefers microtubules over free tubulin. (*A*) K40 of α-tubulin is the sole site of acetylation by αTAT1. 5 μM αTAT1[2-236] was incubated for 1 h at 37 °C with 4 μM axonemal tubulin purified from either WT or α-tubulin[K40R] *Tetrahymena* strains and samples processed as in Fig. 1*B*. Because of high levels of αK40Ac in axonemal microtubules, radiolabel incorporation is less efficient than when using bovine brain tubulin as a substrate. However, no radiolabel incorporation was found after a 3-mo exposure to phosphor screen when α-tubulin[K40R] was used as a substrate. (*B*) αTAT1 exhibits strict substrate specificity for tubulin vs. histones. Reaction mixtures contained [^{14}C]acetylCoA and various combinations of αTAT1[2-236] (4 μM), tubulin, HAT1/RbAp46, and histones H3/H4 and were incubated at 37 °C for 1 h. Even in the presence of very high concentrations of αTAT1 enzyme, histone H3/H4 did not serve as an acetylation substrate, whereas HAT1/RbAp46 acetylated histone H4 under the same experimental conditions. (*C*) αTAT1 displayed a greater catalytic efficiency for taxol-stabilized microtubules than for free tubulin. A range of substrate concentrations straddling the K_m value were incubated for 30 min at 22 °C with 1 μM αTAT1, [^{3}H]acetylCoA, and GTP (microtubules) or GDP (tubulin) and radiolabel incorporation measured with the filter assay. Time-course experiments indicated that the reaction proceeds linearly for the first hour (Fig. 1*C*). Data were fitted to the Michaelis–Menten equation by nonlinear least-square regression. Tubulin was fully polymerized in the microtubule sample and fully depolymerized in the free tubulin sample, as determined in spindown assays (Fig. S1*B*). A larger version of the tubulin saturation curve is shown in Fig. S1*C*. Reactions performed in triplicate. Error bars represent SD and are smaller than some symbols.

αTAT1 Exhibits Substrate Specificity for Tubulin in the Polymerized Form. Microtubule acetylation takes place after microtubule assembly (18, 19). It is therefore thought that the αK40 TAT preferentially targets tubulin in the polymerized state. Substrate saturation curves showed that αTAT1 follows a classic Michaelis–Menten behavior using both free tubulin and taxol-stabilized microtubules as substrates (Fig. 2*C*). Surprisingly, although the K_m values for tubulin and microtubules were not significantly different, the turnover rate (k_{cat}) of αTAT1 for microtubules was more than sixfold greater than for free tubulin. Thus, αTAT1 preferentially acetylates polymerized microtubules over free tubulin at saturating substrate concentrations. Given that tubulin concentration varies between 20 and 200 μM in cells (20) and that nearly 40% of tubulin is polymerized in cells (Fig. 3*H*), αTAT1 is expected to operate at saturating substrate concentrations in vivo and to preferentially acetylate microtubules over free tubulin inside cells.

We note that the turnover rate of αTAT1 is extremely low (k_{cat} for microtubules = 2.2 h^{-1}) and αTAT1 will therefore require tens of minutes to efficiently acetylate microtubules. In mammalian cells, maximum levels of αK40 acetylation require incubations with taxol for several hours (21). Thus, the enzymatic rate constants of αTAT1 fit adequately with the kinetics of tubulin acetylation inside the cell. Finally, we determined the enzymatic constant of αTAT1 for acetyl-CoA (Fig. S1*D*) and found a nearly identical K_m value to the previously purified TAT (22).

αTAT1 Is Necessary and Sufficient to Acetylate α-Tubulin at K40 in Mammalian Cells. Our biochemical findings led us to examine the activity of αTAT1 inside mammalian cells. It is known that PtK2 cells have no detectable α-tubulin K40 acetylation (21). Transient overexpression of αTAT1 in PtK2 cells was sufficient to acetylate nearly all microtubules, whereas catalytically inactive αTAT1 [D157N] or the HAT Elp3 failed to detectably elevate α-tubulin K40 acetylation (Fig. 3 *A* and *B*). Similar results were found in RPE-hTERT cells (Fig. S2). Thus, the catalytic activity of αTAT1 is sufficient to acetylate α-tubulin at K40 in mammalian cells.

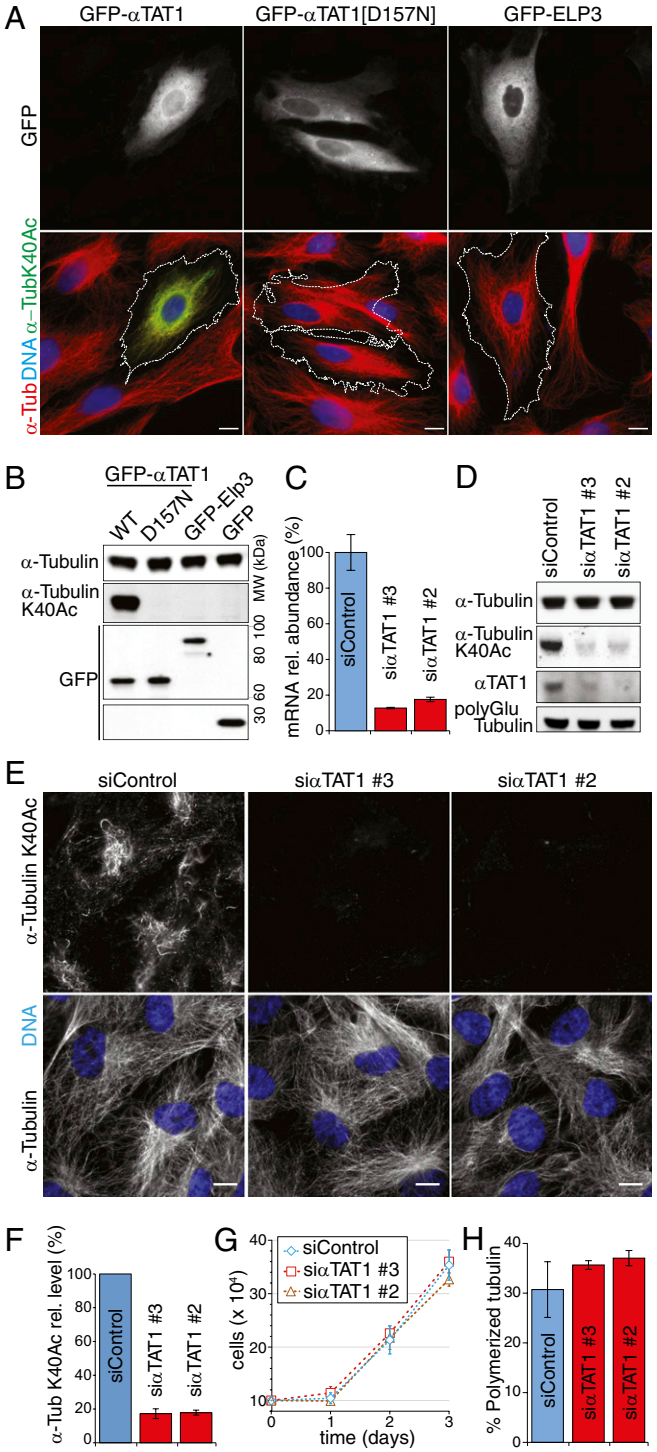

Fig. 3. The enzymatic activity of αTAT1 is necessary and sufficient for acetylation of α-tubulin at lysine 40 in mammalian cells. (*A* and *B*) The enzymatic activity of αTAT1 is sufficient for acetylation of α-tubulin at lysine 40 in PtK2 cells. (*A*) Cells were transfected with GFP-tagged WT αTAT1 (*Left*), αTAT1[D157N] (*Middle*), and ELP3 (*Right*) and stained for DNA (blue), α-tubulin (red), and α-tubulin K40Ac (green). GFP fluorescence was visualized directly. (*B*) Lysates from transfected cells were immunoblotted for the indicated proteins. All GFP fusions are expressed at similar levels. (*C–H*) αTAT1 is required for α-tubulin K40 acetylation in RPE-hTERT cells. (*E*) RPE-hTERT cells were transfected with two independent siRNA duplexes targeting αTAT1 or control siRNA duplexes and stained for the indicated antigens (white) and DNA (blue). (*D*) Lysates from transfected cells were immunoblotted for the indicated antigens. (*C*) αTAT1 mRNA levels were measured by RT-qPCR, and values were normalized to the levels in control siRNA-treated cells. GAPDH was used for intrasample normalization purposes. (*F*) Levels of α-tubulin acetylation at K40 were measured by fluorescent immunoblotting as the ratios of signals for α-tubulin K40Ac over α-tubulin. (*G*) Growth curve was created by measuring the number of cells in each condition starting 48 h after siRNA transfection. (*H*) Amount of polymerized tubulin was measured as fraction of pelletable tubulin in lysates. Error bars correspond to SDs of three independent experiments. (Scale bars, 10 μm.)

Next, we determined the contribution of αTAT1 to microtubule acetylation in RPE-hTERT cells. Two independent siRNA duplexes targeting αTAT1 reduced αTAT1 mRNA and protein by more than 80% (Fig. 3 *C* and *D*). Strikingly, acetylation of α-tubulin at K40 was reduced by more than 80% after depletion of αTAT1, thus indicating the αTAT1 is the major αK40 TAT in mammalian cells (Fig. 3 *D* and *F*). The levels of polyglutamylated tubulin, a marker of ultrastable microtubules found in cilia and centrioles, remained unaffected by αTAT1 depletion (Fig. 3*D*). αTAT1-depleted cells did not exhibit any gross morphological or proliferation defects (Fig. 3 *E* and *G*). Furthermore, αTAT1 depletion did not affect bulk microtubule polymerization, as judged qualitatively by immunofluorescence (Fig. 3*E*) and quantitatively by microtubule spindown assays (Fig. 3*H*). Thus, tubulin acetylation is not required for cell cycle progression or for general microtubule organization.

αTAT1 Promotes Primary Cilium Assembly and Is Conserved in Ciliated Organisms. Given that nearly all αK40 residues are acetylated in ciliary microtubules, and given the association between αTAT1 and the BBSome, we wished to determine the role of αTAT1 in cilium assembly. RPE-hTERT cells assemble a primary cilium when entering quiescence, and we found that αTAT1 depletion significantly delayed assembly of a primary cilia after serum starvation (Fig. 4*A*). We note that although cilium assembly was impaired in αTAT1-depleted cells 12h after serum withdrawal (Fig. 4 *A* and *B* and Fig. S3*A*), cilia were found in nearly equal numbers 24h after serum withdrawal in control or αTAT1-depleted cells (Fig. 4 *A* and *C* and Fig. S3*B*). Cilia assembled in αTAT1-depleted cells contained barely detectable levels of α-tubulin K40 acetylation (Fig. 4C and Fig. S3*B*). Thus, αTAT1 is responsible for α-tubulin K40 acetylation on cytoplasmic as well as ciliary microtubules and αTAT1 facilitates ciliary assembly.

We next examined the phylogenetic distribution of αTAT1. In a survey of 50 genomes of evolutionarily diverse organisms, we found that the presence of a αTAT1 ortholog correlates perfectly with the presence of a cilium or a flagellum (Fig. 4 *D* and *E*, Fig. S4, and Dataset S1). Most remarkably, when we examined the phylogenetic distribution of well-characterized cilia biogenesis factors, such as the BBSsome and the intraflagellar transport (IFT) complexes IFT-A and IFT-B, we found that none of their subunits were better correlated to the presence of a cilium than was αTAT1. Thus, αTAT1 appears to be the molecule whose presence best correlates with the existence of an axoneme.

αTAT Paralogs Are Required for α-Tubulin K40 Acetylation and Touch Sensation in *Caenorhabditis elegans*. Given the broad phylogenetic distribution of αTAT1, we set out to investigate the physiological roles of α-tubulin K40 acetylation using *C. elegans*. The *C. elegans* genome contains a single gene encoding an α-tubulin with a lysine at position 40, *mec-12*, and two genes encoding paralogs of αTAT1, *mec-17* and W06B11.1, which we renamed *atat-2*. As previously reported (23), *mec-17* is expressed exclusively in touch receptor neurons (Fig. 5*A* and Fig. S5A). *atat-2* is expressed not only in touch receptor neurons but also in a subset of ciliated neurons, namely, PDE, ADE, CEP, and OLQ (Fig. 5*A* and Fig. S5*B*). Like the touch receptor neurons, CEP and OLQ are mechanoreceptor neurons activated by external point loads (24, 25). Thus, αK40 acetylation is a feature shared by some, but not all, mechanoreceptor neurons. The restricted expression of *mec-17* and *atat-2* implies that only 12 of 60 of the ciliated sensory neurons in

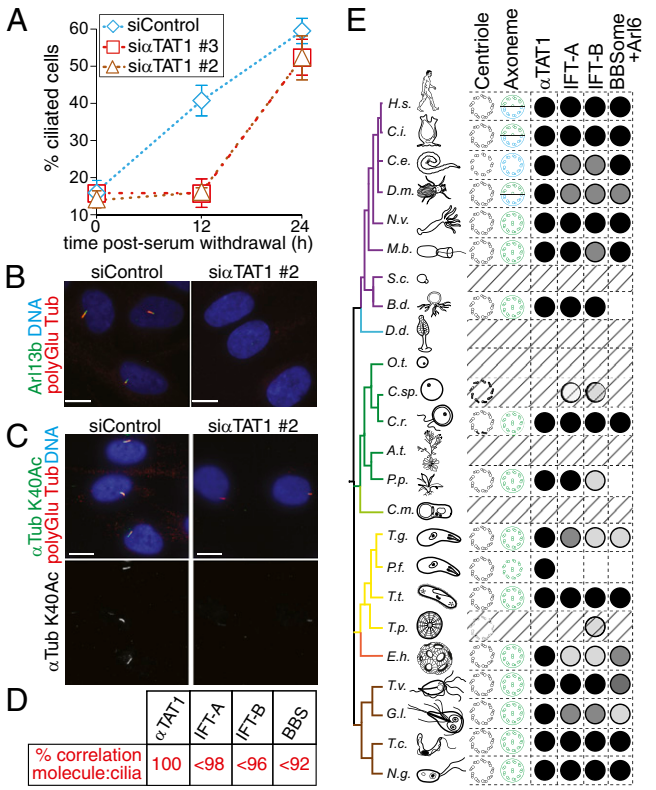

Fig. 4. αTAT1 promotes rapid assembly of the primary cilium. (*A*–*C*) αTAT1 is required for the normal kinetics of primary cilium assembly. (*A*) Following siRNA transfection, cells were serum starved, and polyglutamylated tubulin-positive cilia were counted immediately or after 12 or 24 h. Cilia counts were confirmed by examination of the Arl13b channel. Although the difference in cilia number between control and αTAT1-depleted cells is significant at 12 h postserum starvation ($P < 0.0001$), no significant difference could be detected after 24 h ($P > 0.05$). Error bars represent SDs among three independent experiments. (*B*) Cells fixed 12 h after serum starvation were stained for polyglutamylated tubulin (red), Arl13b (green), and DNA (blue). (*C*) Cells fixed 24 h after serum starvation were stained for polyGlu tubulin (red), α-tubulin K40Ac (green), and DNA (blue). A large proportion of cells are ciliated in the αTAT1-depleted cells. However, α-tubulin K40Ac staining in the cilia of αTAT1-depleted cells is extremely faint. (*D* and *E*) Phylogenetic distribution of αTAT1 compared with IFT-A, IFT-B, BBSome, and Arl6. (*D*) Cilia:molecule correlation coefficients were calculated from Dataset S1 as 100% for αTAT1, 70–98% for IFT-A subunits, 60–96% for IFT-B subunits, and 82–92% for BBSome subunits and Arl6. (*E*) Simplified taxonomic tree, modified from Carvalho-Santos et al. (43). The full name of each organism is shown in Fig. S4. When present in the organism, the basal body structure is diagramed in black, and the cilium is shown in green (motile) or green/blue (motile and primary) or blue (primary). When no cilium is present, hatched bars fill the row. Membrane is omitted for the Plasmodium cilium to represent IFT-independent flagellum assembly. Presence of αTAT1 ortholog is indicated by a black circle. Conservation of IFT-A and IFT-B complexes and BBSome and Arl6 are depicted with shades of gray that correspond to the proportion of subunits present in the organism (black, 100%; dark gray, <100%; medium gray, <60%; and light gray, <30%).

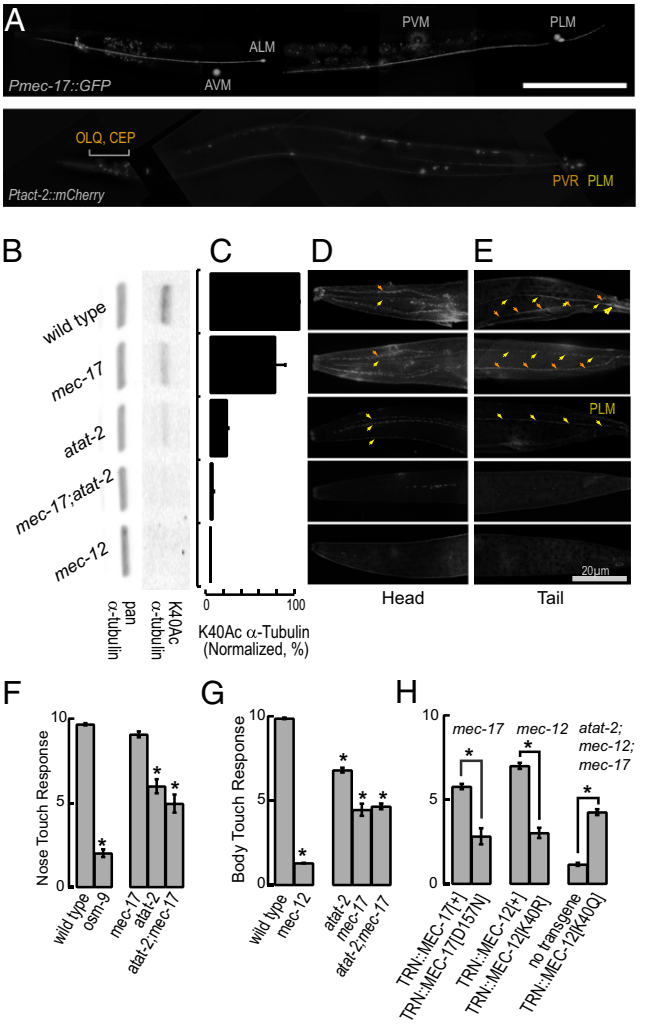

Fig. 5. *C. elegans* mechanosensation requires K40 α-tubulin acetylation. (*A*) P*mec-17*::GFP is expressed only in TRNs (*Upper*), whereas P*atat-2*::mCherry is expressed in TRNs, OLQ, CEP, PVR, and neurons in the ventral nerve cord (*Lower*). (*B* and *C*) Both *mec-17* and *atat-2* are required for α-tubulin K40 acetylation in *C. elegans*. α-Tubulin K40 acetylation is absent in *mec-17;atat-2* double null mutants and *mec-12* α-tubulin null mutants. Bars are normalized to WT intensity ($n = 3$). (*D* and *E*) α-tubulin K40Ac is present in OLQ, CEP, and ALM in the head (*D*) and PVR and PLM in the tail (*E*). For clarity, larger micrographs are shown in. Fig. S5. (*F*) Loss of αTAT-2, but not MEC-17 decreases sensitivity to nose touch ($n = 30$ worms/genotype). *$P < 0.01$ vs. WT, one-way ANOVA $F(4,145) = 154.3$, $P = 10^{-51}$, Tukey post hoc test. (*G*) Loss of both αTAT proteins decreases, but does not eliminate, responses to body touch ($n = 75$ worms per genotype). *$P < 0.01$ vs. WT, one-way ANOVA $F(4,370) = 246.5$, $P = 10^{-103}$, Tukey post hoc test. (*H*) Transgenic expression of WT, but not catalytically inactive MEC-17 or MEC-12[K40R], restores touch sensitivity to *mec-17* and *mec-12* null mutants, respectively (*Left* and *Center*). Transgenic expression of acetyl-mimic MEC-12[K40Q] restores touch sensitivity to *mec-17;atat-2;mec-12* triple null mutants (*Right*) ($n = 75$ worms per genotype). *$P < 0.01$, Student *t* test. Bars in all panels represent mean ± SEM.

C. elegans incorporate acetylated α-tubulin into their microtubules. This further suggests that, as in mammalian cells and *Tetrahymena*, α-tubulin K40 acetylation is dispensable for cilia formation.

Quantitative immunoblotting and immunofluorescence revealed that the levels of MEC-12 α-tubulin K40 acetylation were reduced in *mec-17* and *atat-2* null mutants, and reached undetectable levels in *mec-17;atat-2* double null mutants and a *mec-12* null mutant (Fig. 5 *B*–*E* and Fig. S5 *C* and *D*). Similar effects of the loss of *mec-17*, *atat-2*, and *mec-12* on αK40Ac immunoreactivity were recently reported (15, 26). [MEC-12 is the sole *C. elegans* α-tubulin with a lysine at position 40 (5)]. Thus, the two αTAT1 paralogs appear to account for most, if not all, α-tubulin K40 acetylation in *C. elegans*. Robust α-tubulin K40 acetylation was detected in the TRNs and PVR, as reported previously (5, 27). The CEP and OLQ neurons also contain acetylated microtubules (Fig. 5*C* and Fig. S5*C*), but this modification was not detected in the ciliated chemosensory neurons in the head. TRNs lacking *mec-17* or *atat-2* have decreased levels of α-tubulin K40 acetylation, and loss of both genes reduces α-tubulin K40 acetylation to undetectable levels. α-Tubulin K40 acetylation in CEP or OLQ depends on *atat-2*, but is independent of *mec-17* (Fig. 5*D* and Fig. S5*D*).

Consistent with the expression of *atat-2*, but not *mec-17,* in OLQ, nose touch sensation was significantly reduced in *atat-2* and *mec-17;atat-2* mutants but not in *mec-17* single null mutants (Fig. 5*F*). The OLQ neurons act together with ASH and FLP to mediate avoidance of nose touch (28). Of these three ciliated mechanoreceptor neurons, only OLQ expresses an *atat* gene and contains acetylated α-tubulin (Fig. 5 *A* and *D*). Because CEP neurons are mechanoreceptors that mediate food-induced slowing (29), we measured the speed of *atat-2* mutants off and on bacterial food. *atat-2* mutants move more slowly off food than WT animals (0.14 ± 0.02 and 0.09 ± 0.01 mm/s in WT and *atat-2* mutants, respectively), but retain the ability to slow when encountering a bacterial lawn. Thus, *atat-2* has a role in locomotion, although the *atat-2*-expressing neurons responsible for this phenotype remain to be determined.

When we tested the body touch response that relies on TRN function, we found that *mec-17* and *atat-2* single mutants as well as *mec-17;atat-2* mutants were partially touch insensitive or Mec (Fig. 5*G*). Consistent with the first report of a *mec-17* missense allele (30), the morphology of TRNs was not dramatically altered in any of these mutants, as judged by imaging transgenic animals in which TRNs were labeled with GFP (Fig. S6). The Mec phenotype was more severe in *mec-17* than in *atat-2* mutants, but less severe than in the *mec-12* mutant. The variation in the severity of the behavioral phenotype correlated with the level of αK40Ac immunoreactivity detected in the TRNs (Fig. S7). The mild phenotype of the double mutant that lacks α-tubulin K40 acetylation entirely suggests that although this posttranslational modification is important for touch sensitivity, it is not essential. We note that Akella et al. (15) reported that *mec-17;atat-2* double mutants were more severely Mec. The discrepancy may reflect a difference in the preparation of the deletion mutants, which were outcrossed before use in the present study. Although it is not yet clear how loss of K40 acetylation disrupts touch sensation, it is unlikely to act by altering the growth or development of the TRNs.

To test whether the role of αTAT1 in touch sensation depends on its ability to acetylate MEC-12 α-tubulin at K40, we genetically manipulated both the enzyme and its substrate. Transgenic *mec-17* mutants expressing MEC-17[+] were significantly more touch sensitive than those expressing the catalytically inactive MEC-17[D157N] (Fig. 5*H*). Similarly, *mec-12* mutants expressing MEC-12[+] α-tubulin were significantly more touch sensitive than those expressing the nonacetylatable MEC-12[K40R] α-tubulin. We note that *mec-17*;MEC-17[+] and *mec-12*;MEC-12[+] transgenic animals were less touch sensitive than wild-type animals. We suspect that this is an artifact of overexpression of UNC-86::MEC-3 binding sites, as this manipulation is known to decrease expression of multiple genes critical for touch receptor neuron function (31). [The *mec-17* promoter used to direct expression of all transgenic proteins to the TRNs contains two binding sites (23).] Nevertheless, these results indicate that acetylation of MEC-12 α-tubulin at K40 is required for full sensitivity to gentle touch, and suggest that artificial acetylation of MEC-12 α-tubulin should bypass the need for *mec-17* and *atat-2*. We tested this idea by expressing the acetyl-mimic MEC-12 [K40Q] α-tubulin, and found that this transgene was sufficient to partially restore touch sensation to *mec-17;atat-2;mec-12* triple mutants (Fig. 5*H*).

Discussion

Using a combination of in vitro biochemistry and cell-based studies, we and others (15) have shown that αTAT1 (C6orf134) is a bona fide TAT. We additionally show that recombinant αTAT1 efficiently deposits acetyl groups on K40 of α-tubulin in vitro, that this activity is associated with the conserved GNAT-like domain and is abrogated in a αTAT1[D157N] mutant, and that αTAT1 is highly specific for tubulin over histones. Active αTAT1, but not catalytically dead αTAT1[D157N], is sufficient to produce acetylated microtubules in PtK2 cells which lack endogenous acetylated tubulin. TAT proteins are necessary for the production of acetylated tubulin in mammalian cells and *C. elegans*. Recent studies have suggested that Elp3 also functions as an αK40 TAT (8, 27). Although Elp3 may indirectly influence microtubule acetylation, we report that Elp3 fails to detectably acetylate microtubules in PtK2 cells. Because *C. elegans* TRNs retain acetylated microtubules and wild-type touch sensitivity in *elpc-3* null mutants (27), Elp3 is unlikely to be a major contributor to microtubule acetylation in vivo. Thus, we propose that αTAT1 is the major, and possibly only, αK40 TAT.

Acetylation of α-Tubulin K40 by αTAT1 Inside the Microtubule Lumen. The intralumenal location of αK40 poses a significant accessibility problem for αTAT1. An initial model proposes that αTAT1 (measured Stokes radius R_S = 3.5 nm) enters the microtubule through the 14-nm diameter open ends, and is then restricted by unidimensional diffusion inside the lumen to reach its substrate. However, the nearly indistinguishable K_m of αTAT1 for tubulin and microtubules strongly suggests that αK40 is freely accessible to αTAT1 in microtubules. How could αTAT1 possibly reach its intralumenal substrate in an unrestricted manner?

The small molecule taxol (R_S = 0.8 nm) also binds to a site within the microtubule lumen. Surprisingly, taxol binding to microtubules is limited only by 3D diffusion and does not vary along the length of microtubules (32), thus implying that the taxol binding site is freely accessible. One idea is that taxol enters via 17-Å pores between protofilaments. Another is that lateral interactions between protofilaments are sufficiently weak to allow large openings to continuously appear and close in the microtubule wall (32). This microtubule "breathing" model is supported by cryo-electron microscopy observations of lattice defects and by the finding that microtubules rapidly change the number of their protofilaments in response to taxol binding (33). Because αTAT1 cannot enter through the 17-Å pores, it most likely accesses its substrate by entering through the transient lateral openings, and may therefore enable a quantitative study of microtubule breathing.

Somewhat surprisingly, the preference of αTAT1 for polymerized tubulin manifests itself in an increased k_{cat} rather than a decreased K_m. Because the immediate vicinity of K40 is resolved in the crystal structure of tubulin dimers (34) but not in the structure of microtubules (35), the K40 loop is likely more flexible and thus more prone to adopt a conformation optimal for catalysis in microtubules than in free tubulin. Beyond the preference of αTAT1 for microtubules vs. free tubulin, a major question relates to how αTAT1 might be directed to specific regions of a given microtubule within the cell. Indeed, α-tubulin K40Ac staining along cytoplasmic microtubules is often quite discontinuous (19) (Figs. 3*E* and 5 *C* and *D*), whereas tubulin detyrosination is seen all along the length of stable microtubules (36). Perhaps the acetylated regions are those that were bent the most and thus provided the greatest substrate accessibility to αTAT1 through increased breathing.

Acetylation of α-Tubulin K40 and Cilium Assembly. In *Chlamydomonas*, *Tetrahymena* and *C. elegans*, α-tubulin K40 acetylation is dispensable for cilium or flagellum assembly. However, in mammalian cells, we find that the normal kinetics of cilium assembly require αTAT1. This is unlikely to be a consequence of siRNA off-target effects, as we confirmed these results using two independent siRNA duplexes. Likewise, we used two independent markers of cilia, polyglutamylated tubulin and Arl13b (Fig. 4*B*). Although it is conceivable that delays in the kinetics of flagellum assembly have been overlooked in previous experiments, it is equally likely that the assembly of mammalian primary cilia is more sensitive to the loss of α-tubulin K40 acetylation than in other organisms. Our results are also consistent with the findings that HDAC6 entry into cilia triggers cilium disassembly (37). A unique feature of mammalian primary cilia is their regulated emergence and resorption in quiescent vs. proliferating cells. Thus, an appealing hypothesis is that α-tubulin K40 acetylation of axonemal microtubules serves to couple the cycle of cilium emergence and resorption to the cell division cycle (38). Indeed, whereas most cells resorb their cilium in G1/S by shortening the axoneme, Ptk1 cells (which lack

α-tubulin K40 acetylation) resorb their cilium in mitotic prophase by releasing the entire axoneme into the cytoplasm (39). Coupling cilium assembly to the cell cycle is likely important in neuroepithelial cells, which must respond to Hedgehog using their primary cilium while actively dividing. More generally, cilium assembly and resorption may be linked to oncogenic transformation and alteration in signaling responsiveness (40).

Acetylated Microtubules Are Essential for Normal Touch Sensation in *C. elegans*. *C. elegans* hermaphrodites have 30 predicted mechanoreceptor neurons (41), and at least 14 of them express either *mec-17* or *atat-2*. Thus, although acetylated tubulin is a common feature of mechanoreceptor neurons, it does not appear to be universal. For example, αTAT-2 expression and acetylated tubulin staining are found in OLQ but not ASH or FLP, but these sensory neurons mediate avoidance to nose touch in parallel (28).

The touch receptor neurons coexpress *mec-17* and *atat-2*. Loss of one or both genes induces a partial defect in touch sensitivity. This defect can be partially restored by transgenic expression of MEC-17[+] but not catalytically dead MEC-17. Similarly, loss of MEC-12 induces a profound loss of touch sensitivity that can be partially restored by expression of MEC-12[+] but not an acetylation resistant MEC-12. The mild defect observed in *mec-17; atat-2* double mutants was enhanced in a *mec-12;mec-17;atat-2* triple mutant that lacks both αTAT activities and their α-tubulin substrate. Consistent with the idea that modified α-tubulin per se is required for touch sensation, the severe touch insensitivity of the triple mutant was partially restored by transgenic expression of MEC-12[K40Q], an α-tubulin allele that is predicted to mimic α-tubulin acetylated at K40.

In conclusion, the identification of αTAT1 as an αK40 TAT will enable further investigation of the physiology, biochemistry, and biophysics of α-tubulin K40 acetylation.

Materials and Methods

General Methods, Antibodies, DNA Constructs, and *C. elegans* Strains. Recombinant protein expression and purification, microtubule purification, acetyltransferase assays, cell culture, immunofluorescence microscopy, siRNA-mediated αTAT1 depletion, phylogenetic analysis, generation of transgenic *C. elegans* strains, and *C. elegans* behavioral assays are described in *SI Materials and Methods*. Reagents used in this study are also described in *SI Materials and Methods*.

ACKNOWLEDGMENTS. We thank Julie Theriot, Aaron Straight, and Joanna Wysocka (Stanford University, Stanford, CA); Martin Gorowski (Rochester University, Rochester, NY); Alain Chariot and Laurent Ngyunen (Liège University, Wallonia, Belgium); Carsten Janke (Institut Curie, Orsay, France); Kenji Kontani (University of Tokyo, Tokyo) for reagents; Cen Gao for worm injection; and J. Fernando Bazan for uncovering the GNAT fold in C6orf134. Some nematode strains used in this work were provided by Martin Chalfie, Cornelia I. Bargmann, and the Caenorhabditis Genetics Center, which is funded by the National Institutes of Health, National Center for Research Resources. This work was supported by National Institutes of Health Grants GM089933 (to M.V.N.) and NS047715 and EB006745 (to M.B.G.).

1. Hammond JW, Cai D, Verhey KJ (2008) Tubulin modifications and their cellular functions. *Curr Opin Cell Biol* 20:71–76.
2. Nogales E, Wolf SG, Downing KH (1998) Structure of the alpha beta tubulin dimer by electron crystallography. *Nature* 391:199–203.
3. Gaertig J, et al. (1995) Acetylation of lysine 40 in alpha-tubulin is not essential in Tetrahymena thermophila. *J Cell Biol* 129:1301–1310.
4. Kozminski KG, Diener DR, Rosenbaum JL (1993) High level expression of non-acetylatable alpha-tubulin in Chlamydomonas reinhardtii. *Cell Motil Cytoskeleton* 25: 158–170.
5. Fukushige T, et al. (1999) MEC-12, an alpha-tubulin required for touch sensitivity in C. elegans. *J Cell Sci* 112:395–403.
6. Reed NA, et al. (2006) Microtubule acetylation promotes kinesin-1 binding and transport. *Curr Biol* 16:2166–2172.
7. Cai D, McEwen DP, Martens JR, Meyhofer E, Verhey KJ (2009) Single molecule imaging reveals differences in microtubule track selection between Kinesin motors. *PLoS Biol* 7:e1000216.
8. Creppe C, et al. (2009) Elongator controls the migration and differentiation of cortical neurons through acetylation of alpha-tubulin. *Cell* 136:551–564.
9. Ohkawa N, et al. (2008) N-acetyltransferase ARD1-NAT1 regulates neuronal dendritic development. *Genes Cells* 13:1171–1183.
10. Shen Q, et al. (2009) NAT10, a nucleolar protein, localizes to the midbody and regulates cytokinesis and acetylation of microtubules. *Exp Cell Res* 315:1653–1667.
11. Loktev AV, et al. (2008) A BBSome subunit links ciliogenesis, microtubule stability, and acetylation. *Dev Cell* 15:854–865.
12. Jin H, et al. (2010) The conserved Bardet-Biedl syndrome proteins assemble a coat that traffics membrane proteins to cilia. *Cell* 141:1208–1219.
13. Steczkiewicz K, Kinch L, Grishin NV, Rychlewski L, Ginalski K (2006) Eukaryotic domain of unknown function DUF738 belongs to Gcn5-related N-acetyltransferase superfamily. *Cell Cycle* 5:2927–2930.
14. LeDizet M, Piperno G (1987) Identification of an acetylation site of Chlamydomonas alpha-tubulin. *Proc Natl Acad Sci USA* 84:5720–5724.
15. Akella JS, et al. (2010) MEC-17 is an alpha-tubulin acetyltransferase. *Nature* 467: 218–222.
16. Choudhary C, et al. (2009) Lysine acetylation targets protein complexes and co-regulates major cellular functions. *Science* 325:834–840.
17. Marmorstein R, Trievel RC (2009) Histone modifying enzymes: Structures, mechanisms, and specificities. *Biochim Biophys Acta* 1789:58–68.
18. L'Hernault SW, Rosenbaum JL (1983) Chlamydomonas alpha-tubulin is post-translationally modified in the flagella during flagellar assembly. *J Cell Biol* 97:258–263.
19. Webster DR, Borisy GG (1989) Microtubules are acetylated in domains that turn over slowly. *J Cell Sci* 92:57–65.
20. Hiller G, Weber K (1978) Radioimmunoassay for tubulin: A quantitative comparison of the tubulin content of different established tissue culture cells and tissues. *Cell* 14: 795–804.
21. Piperno G, LeDizet M, Chang XJ (1987) Microtubules containing acetylated alpha-tubulin in mammalian cells in culture. *J Cell Biol* 104:289–302.
22. Maruta H, Greer K, Rosenbaum JL (1986) The acetylation of alpha-tubulin and its relationship to the assembly and disassembly of microtubules. *J Cell Biol* 103:571–579.
23. Zhang Y, et al. (2002) Identification of genes expressed in C. elegans touch receptor neurons. *Nature* 418:331–335.
24. Kang L, Gao J, Schafer WR, Xie Z, Xu XZ (2010) C. elegans TRP family protein TRP-4 is a pore-forming subunit of a native mechanotransduction channel. *Neuron* 67:381–391.
25. Kindt KS, et al. (2007) Caenorhabditis elegans TRPA-1 functions in mechanosensation. *Nat Neurosci* 10:568–577.
26. Bounoutas A, O'Hagan R, Chalfie M (2009) The multipurpose 15-protofilament microtubules in C. elegans have specific roles in mechanosensation. *Curr Biol* 19: 1362–1367.
27. Solinger JA, et al. (2010) The Caenorhabditis elegans Elongator complex regulates neuronal alpha-tubulin acetylation. *PLoS Genet* 6:e1000820.
28. Kaplan JM, Horvitz HR (1993) A dual mechanosensory and chemosensory neuron in Caenorhabditis elegans. *Proc Natl Acad Sci USA* 90:2227–2231.
29. Sawin ER, Ranganathan R, Horvitz HR (2000) C. elegans locomotory rate is modulated by the environment through a dopaminergic pathway and by experience through a serotonergic pathway. *Neuron* 26:619–631.
30. Chalfie M, Au M (1989) Genetic control of differentiation of the Caenorhabditis elegans touch receptor neurons. *Science* 243:1027–1033.
31. Toms N, Cooper J, Patchen B, Aamodt E (2001) High copy arrays containing a sequence upstream of mec-3 alter cell migration and axonal morphology in C. elegans. *BMC Dev Biol* 1:2–17.
32. Díaz JF, Barasoain I, Andreu JM (2003) Fast kinetics of Taxol binding to microtubules. Effects of solution variables and microtubule-associated proteins. *J Biol Chem* 278: 8407–8419.
33. Díaz JF, Valpuesta JM, Chacón P, Diakun G, Andreu JM (1998) Changes in microtubule protofilament number induced by Taxol binding to an easily accessible site. Internal microtubule dynamics. *J Biol Chem* 273:33803–33810.
34. Gigant B, et al. (2000) The 4 A X-ray structure of a tubulin:stathmin-like domain complex. *Cell* 102:809–816.
35. Nogales E, Whittaker M, Milligan RA, Downing KH (1999) High-resolution model of the microtubule. *Cell* 96:79–88.
36. Geuens G, et al. (1986) Ultrastructural colocalization of tyrosinated and detyrosinated alpha-tubulin in interphase and mitotic cells. *J Cell Biol* 103:1883–1893.
37. Pugacheva EN, Jablonski SA, Hartman TR, Henske EP, Golemis EA (2007) HEF1-dependent Aurora A activation induces disassembly of the primary cilium. *Cell* 129: 1351–1363.
38. Seeley ES, Nachury MV (2010) The perennial organelle: Assembly and disassembly of the primary cilium. *J Cell Sci* 123:511–518.
39. Jensen CG, Davison EA, Bowser SS, Rieder CL (1987) Primary cilia cycle in PtK1 cells: Effects of colcemid and taxol on cilia formation and resorption. *Cell Motil Cytoskeleton* 7:187–197.
40. Seeley ES, Carrière C, Goetze T, Longnecker DS, Korc M (2009) Pancreatic cancer and precursor pancreatic intraepithelial neoplasia lesions are devoid of primary cilia. *Cancer Res* 69:422–430.
41. Goodman MB (2006) Mechanosensation. *WormBook*, ed The *C. elegans* Research Community, WormBook. Available at http://www.wormbook.org.
42. Eddé B, et al. (1990) Posttranslational glutamylation of alpha-tubulin. *Science* 247: 83–85.
43. Carvalho-Santos Z, et al. (2010) Stepwise evolution of the centriole-assembly pathway. *J Cell Sci* 123:1414–1426.